Exchange Properties of the Three-Dimensional Coordination Compound 1,3,5-Tris(4-ethynylbenzonitrile)benzene·AgO_3SCF_3

Geoffrey B. Gardner,[†] Y.-H. Kiang,[†] Stephen Lee,*[,†] Anil Asgaonkar,[†] and D. Venkataraman[‡]

Contribution from the Department of Chemistry, University of Michigan, Ann Arbor, Michigan 48109-1055, and Department of Chemistry, University of Illinois, Urbana, Illinois 61801

Received February 23, 1996[⊗]

Abstract: Properties such as guest removal and exchange within a host crystal are investigated for benzene·1,3,5-tris(4-ethynylbenzonitrile)(**1**)·silver triflate(AgOTf) (polymorph A). The 15 Å × 22 Å channels in the crystal structure are retained through both guest exchange and complete guest removal. The apohost (defined to be a host without guests system) exhibits selectivity for new guests by absorbing aromatic molecules (ranging from 1.5−4 guests per molecule of **1**) and not aliphatic molecules from the vapor phase. In solution, guests such as toluene, undecane, and benzyl alcohol are shown to be accomodated typically with two to three guest molecules for every molecule of **1**. Guest exchange of nonfunctionalized aliphatic and aromatic molecules make no changes in the original benzene·**1**·AgOTf adduct orthorhombic cell parameters (11.625(3) Å × 19.110(7) Å × 38.856(15) Å) greater than 0.4 Å for any axis. However, crystals containing alcoholic aromatic molecules can be indexed to the two-dimensional rectangular analog of an orthorhombic cell, with *b* and *c* cell axis of 22.0−22.5 Å and 32.8−34.7 Å, respectively. Complete evacuation of the channels by heating also produces a two-dimensional rectangular cell with parameters 22.76(2) Å × 36.32(3) Å. X-ray powder diffraction of all adducts demonstrates the retention of the original three-dimensional $ThSi_2$-type network or, in the case of the alcoholic adduct or apohost systems, the two-dimensional projection of this channel structure. Repeated removal and reintroduction of benzyl alcohol guests is demonstrated to occur with the retention of crystallinity and without the macroscopic reformation of the crystallites.

Introduction

There has recently been renewed interest in the synthesis of mainly organic systems with materials properties such as porosity and guest exchangeability, traditionally associated with inorganic zeolites.[1−7] Such synthetic strategies typically involve assembly using a modular "building-block" approach whereby organic portions of the structure are constructed as supramolecular fragments and subsequently assembled together in the formation of a porous solid.[8,9] However, one general defect with this approach has been that such systems, upon removal of the included guest, often undergo phase transitions to other more dense packings.[1,2,10−12]

One of the reasons for this difficulty may lie in the nature of the intermolecular forces. In many of the previously studied systems, the crucial intermolecular bonds have been hydrogen bonds.[13−17] While some workers have shown that hydrogen bonds in systems such as Dianin's compound can be strong enough to compete with the very unfavorable van der Waals packing forces of the true porous system,[18,19] these are the exceptions rather than the rule.[2] Consequently, the substitution of an even stronger interfragment bond is still desirable. Earlier work has indeed shown that the stronger coordination bond based systems allows for the partial or complete removal of guests.[5,6,20,21]

In this article, we report for a three-dimensional framework system based on coordination bonds that complete and nonde-

* Author to whom correspondence should be addressed.
[†] University of Michigan.
[‡] University of Illinois.
[⊗] Abstract published in *Advance ACS Abstracts,* July 1, 1996.

(1) Hoskins, B. F.; Robson, R. *J. Am. Chem. Soc.* **1990**, *112*, 1546−1554.
(2) Wang, X.; Simard, M.; Wuest, J. D. *J. Am. Chem. Soc.* **1994**, *116*, 12119−12120.
(3) Fujita, M.; Kwon, Y. J.; Washizu, S.; Ogura, K. *J. Am. Chem. Soc.* **1994**, *116*, 1151−1152.
(4) Gardner, G. B.; Venkataraman, D.; Moore, J. S.; Lee, S. *Nature* **1995**, *374*, 792−795.
(5) Venkataraman, D.; Gardner, G.; Lee, S.; Moore, J. S. *J. Am. Chem. Soc.* **1995**, *117*, 11600−11601.
(6) Yaghi, O. M.; Li, G.; Li, H. *Nature* **1995**, *378*, 703−706.
(7) Yaghi, O. M.; Li, H. *J. Am. Chem. Soc.* **1996**, *188*, 295−296.
(8) Simard, M.; Su, D.; Wuest, J. D. *J. Am. Chem. Soc.* **1991**, *113*, 4696−4698.
(9) Kaszynski, P.; Friedli, A. C.; Michl, J. *J. Am. Chem. Soc.* **1992**, *114*, 601−620.
(10) Venkataraman, D.; Lee, S.; Zhang, J.; Moore, J. S. *Nature* **1994**, *371*, 591−593.
(11) Endo, K.; Sawaki, T.; Koyanagi, M.; Kobayashi, K.; Masuda, H.; Aoyama, Y. *J. Am. Chem. Soc.* **1995**, *117*, 8341−8352.
(12) Abrahams, B. F.; Hoskins, B. F.; Michail, D. M.; Robson, R. *Nature* **1994**, *369*, 727−729.
(13) Subramanian, S.; Zaworotko, M. J. *Coord. Chem. Rev.* **1994**, *137*, 357−401.
(14) *Inclusion Compounds*; Atwood, J. L., Davies, J. E. D., MacNicol, D. D., Eds.; Academic Press: London, 1984; Vol. 1−2.
(15) Ermer, O.; Lindenberg, L. *Helv. Chim. Acta* **1991**, *74*, 825−877.
(16) Etter, M. C. *Acc. Chem. Res.* **1990**, *23*, 120−126.
(17) Fan, E. K.; Yang, J.; Geib, S. J.; Hopkins, M. D.; Hamilton, A. D. *J. Chem. Soc., Chem. Commun.* **1995**, 1251−1252.
(18) Ung, A. T.; Gizachew, D.; Bishop, R.; Scudder, M. L.; Dance, I. G. *J. Am. Chem. Soc.* **1995**, *117*, 8745−8756.
(19) Lee, F.; Gabe, E.; Tse, J. S.; Ripmeester, J. A. *J. Am. Chem. Soc.* **1988**, *110*, 6014−6019.
(20) The earliest and one of the most widely studied of such coordination bond solids are the Hofmann clathrates (e.g., $Ni(NH_3)_2Ni(CN)_4·2C_6H_6$). These have been reviewed in vol. 1, pp 29−57 of ref 14 by T. Iwamoto. It is noted that "in spite of the earlier discussion which suggested high stability of Hofmann's clathrates, Hofmann type inclusion compounds decompose gradually under ambient conditions by releasing the guest molecules". Indeed, as stated in the review, one of the few well characterized Hofmann compounds with no guests ($Cd(N(CH_3)_3)_2Ni(CN)_4$ forms an interlocking structure for which no inclusion compounds have yet been obtained.
(21) A cyanide salt which retains its crystal structure upon evaporation of solvent is $K_2Zn_3[Fe(CN)_6]·xH_2O$. See: Cartaud, P.; Cointot, A.; Renaud, A. *J. Chem. Soc., Faraday Trans. 1* **1981**, *77*, 1561.

S0002-7863(96)00595-1 CCC: $12.00

structive removal of all included guest molecules are possible through removal of guests by evaporation. The pore diameters of 15−20 Å are to our knowledge the largest cavities which can be sustained in the absence of guests for any organic coordination or hydrogen bonded solids.

Experimental Procedure

1,3,5-Tris(4-ethynylbenzonitrile)benzene, **1**, was prepared as previously described.[4] All materials were purchased from Aldrich Chemical Company and used without further purification.

Elemental analysis was performed on a Perkin-Elmer 2400 CHN Analyzer. Thermogravimetric analysis (TGA) and differential scanning calorimetry (DSC) were performed on the Perkin-Elmer 7 Thermal Analysis series. Both TGA and DSC were performed under nitrogen flow and at a scan rate of 10 °C/min. DSC was performed in aluminum pans.

Powder X-ray diffraction data were recorded on an Enraf-Nonius Guinier camera at 40 kV, 13 mA for $CuK_{\alpha 1}$; $\lambda = 1.5404$ Å, with an internal standard of $RbZn_4Ga_5S_{12}$.[22] Lattice constants were fitted and powder data were indexed by a least squares method. Theoretical powder patterns were generated with the aid of the program Cerius^2.[23] Solution exchange sample preparation for the Guinier camera was as follows: A borosilicate capillary was filled with the guest molecule, either neat as solvent or dissolved in a known minimum of toluene. Microcrystalline powder of **1**·AgOTf grown in benzene was suspended in the guest solution for 15 to 60 min before the tube was sealed. The capillary was then mounted on the Guinier camera and exposed to X-rays for a period of 6−12 h. Powder X-ray diffraction data of the guest-free host was recorded on an Rigaku Rotaflex diffractometer at 60 kV, 180 mA for $CuK_{\alpha 1}$; $\lambda = 1.5404$ Å, with an internal Si standard. Scan speed was at 1°/min with a step size of 0.01° in 2θ.

Crystalline size was determined by optical microscopy on a Leitz Orthoplux IIPOL-BK and Panasonic Olympus BH2-UMA.

All ^{1}H NMR spectra were recorded on a Bruker AC-200, AM-300, or AM-360.

Solution Exchange. Sample preparation for the solution exchange ^{1}H NMR experiment was as follows: The benzene grown crystals of **1**·AgOTf were initially washed with toluene at room temperature (about 1 mL for every 20 mg) and gravity filtered until the supporting filter paper was just slightly damp. The crystals were then soaked in a solution of guest molecules either neat or in a known minimum of toluene at room temperature. After 2 h, the crystals were vacuum filtered until the supporting filter paper appeared visually dry. In addition, if the guest was alcoholic, the crystals were further washed with approximately 1 mL of toluene at −40 °C and suctioned until dry. The material was then dissolved in acetone-d_6, and the ratio of guest:**1** was determined. Standard deviations for these values were obtained by repeated measurements. Sample preparation of the 1,3,5-tricyanobenzene·AgOTf crystals was identical to that of **1**·AgOTf except for the initial wash with toluene at room temperature. As noted in the text, for certain experiments the morphology of the original crystals of **1**·AgOTf was optically monitored on crystals of approximately 1 mm × 0.5 mm × 0.5 mm.

Vapor Exchange. Vapor exchange sample preparation for the TGA and ^{1}H NMR was as follows: The crystals grown in benzene were first gravity filtered until the supporting filter paper was slightly damp. The sample was then immediately placed in the thermogravimetric analyzer and heated from room temperature to 200 °C at 10 °C/min to void the solid of initially included solvent. The apohost was then suspended above a solution of the guest molecules, taking care to maintain spatial separation between host and guest and sealed in a vial. The vial was heated 40 to 65 °C for the length of the experiment, typically 12 h. Samples were analyzed by TGA and by ^{1}H NMR through dissolution of the host compound in acetone-d_6. Standard deviations for these values were obtained through repeated measurements. For certain experiments the morphology of the apohost **1**·AgOTf was optically monitored on crystals approximately 0.03 mm × 0.01 mm × 0.01 mm in size.

Results and Discussion

The focus of our investigations was the benzene·1,3,5-tris-(4-ethynylbenzonitrile)(**1**)·silver triflate (AgOTf) adduct.[4] The several features of this structure pertinent to the experiments reported in this paper are highlighted below.

The coordination compound **1**·AgOTf (polymorph A) is an infinite three-dimensional crystalline solid. The nitrile moieties of the trigonal phenylacetylene ligand **1** coordinate end-on to

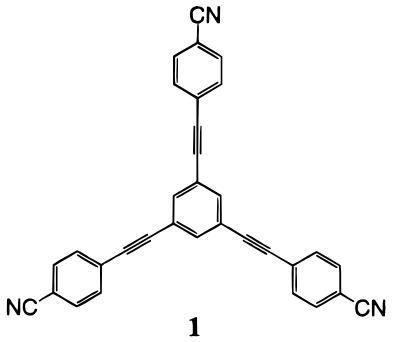

1

the trigonal pyramidal silver cation to form a three-dimensional (3,3)-connected net topologically analogous to the inorganic structure type $ThSi_2$ (Figure 1a).[24] The framework of this solid consists of alternating metal cations and organic ligands. There are six interpenetrated $ThSi_2$-type networks in the final structure.[25] The average face-to-face distance of the phenyl rings between adjacent interpenetrating network is 3.5 Å, a typical distance for a $\pi-\pi$ interaction between aromatic rings.[26] Figure 1b illustrates that the interpenetration of the networks does not interfere with the formation of hexagonal channels. These exceptionally large cavities with cross sections of 15 Å × 22 Å run along the *a* axis. The silver cations lie along the channels where they are coordinatively bound by the silver triflate counterion. The walls of the channels are composed of these cations, the counterions, and phenylacetylene ligands. Benzene molecules from the crystallization process are located within the pores; 12 of these per unit cell could be identified from the Fourier difference map (shown in thick lines in Figure 1b). These benzenes occupy the corners of each of the hexagonal channels and possess much larger thermal ellipsoids than the phenyl rings integrated into the network. Furthermore, the largest residual electron peaks occur in the center of the channels where no molecules have been located crystallographically, suggesting that there are additional highly disordered benzenes occupying this space.

The indication that there were translationally disordered and potentially fluid-like regions in the interior of these large channels suggested several issues for investigation: First, what range of guests could replace the initially included benzene? Second, could the fluid-like region of guest molecules be thermally removed from the channels without destruction of the host network? And third, if guests could be removed, what behavior would the voided solid exhibit when exposed to potential guests?

1. Solution Guest Exchange within a Porous Coordination Compound. We previously communicated results indicating

(22) Schwer, H.; Keller, E.; Krämer, V. *Z. Kristallogr*. **1993**, *204*, 203−213.

(23) CERIUS^2 Chemical Simulations Software Package; Molecular Simulation Inc.; Burlington, MA, 1994.

(24) Wells, A. F. *Structural Inorganic Chemistry*; Oxford University Press: New York, 1993; pp Chapter 3.

(25) Carlucci, L.; Ciani, G.; Proserpio, D. M.; Sironi, A. *J. Am. Chem. Soc*. **1995**, *117*, 4562−4569.

(26) Desiraju, G. R.; Gavezzotti, A. *Acta Crystallogr*. **1989**, *B45*, 473−482.

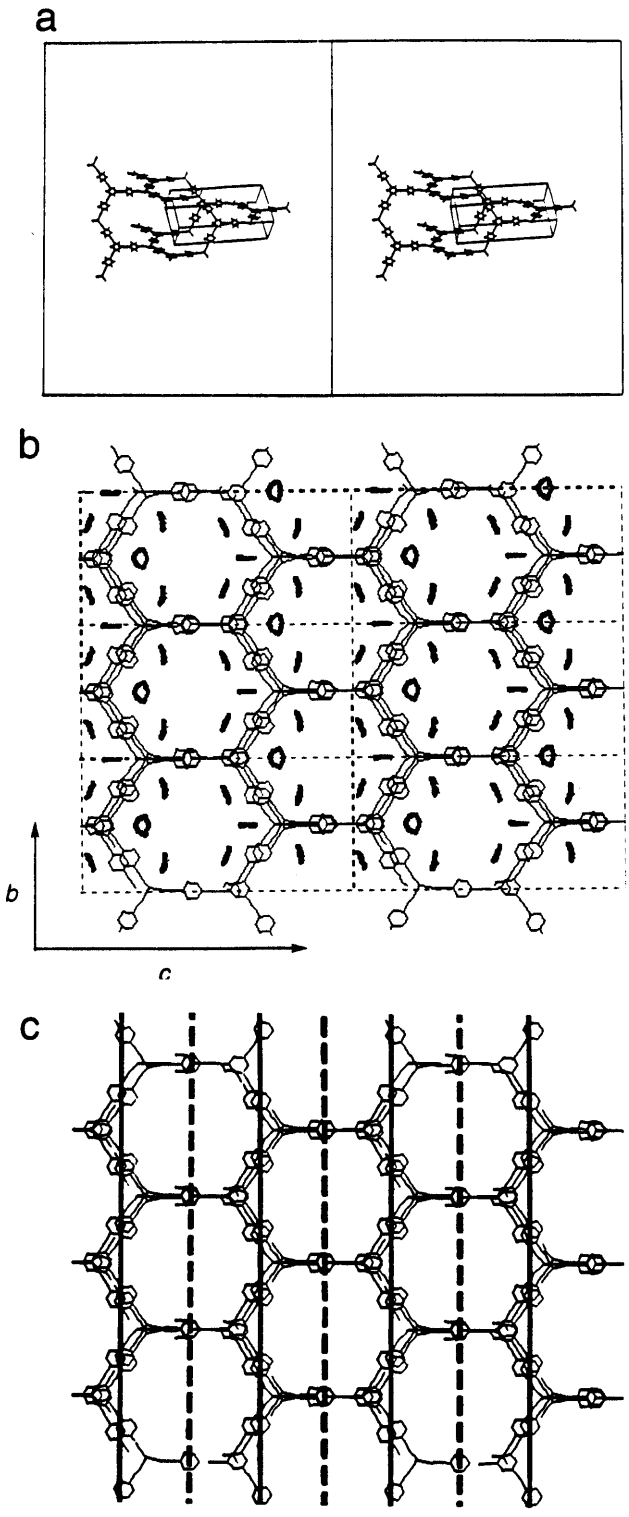

Figure 1. (a) Stereoview of a single $ThSi_2$-type network of the crystal structure of **1**·AgOTf. Five more nets, three per unit cell, interpenetrate to fill the void space created in a singlet net. (b) View of **1**·AgOTf down the *a* axis showing the 15 Å × 22 Å hexagonal channels. Included benzene molecules from crystallization are shown in bold lines in the cavities of the channel. Triflate anions have been omitted for clarity. (c) View of **1**·AgOTf down the *a* axis with plane waves corresponding to the 002 reflection highlighted. Bold solid lines correspond to wave crests, dotted lines to wave troughs. Benzene molecules and triflate anions are omitted for clarity.

a nondestructive solution exchange of guests can take place in **1**·AgOTf.[4] However, the exchange reported involved only the replacement of initially included benzene with benzene-d_6. In order to explore a broader range of guest/host interactions, this exchange study was extended to the series of compounds shown in Table 1. The list of compounds represents a wider array of guests, including aliphatic, aromatic, and aromatic alcoholic molecules. By expanding the list of potential guests, our intention was to determine characteristics of the guest, if any, that influenced solution incorporation into the host.

Solution exchange of guests required immersion of host crystals in a guest solution and analysis of the adduct by ^{1}H NMR. Guest:**1** molar ratios detected after exposure to the guest are tabulated for some of the molecules in Table 1. We report two different values of ratios, each for a different crystallite size **1**·AgOTf. In the column labeled "macrocrystalline ratio", we report the guest:**1** molar ratio for crystals on the order of 1 mm × 0.5 mm × 0.5 mm, while for the column labeled "microcrystalline ratio", we report the guest:**1** molar ratio for crystals approximately 0.03 mm × 0.01 mm × 0.01 mm in size. Of note is the relatively narrow range of values detected. For macrocrystalline exchange, five of these guests fall in a range of about 1.5−3.0 guests for every molecule of **1**, with benzyl alcohol exhibiting the highest guest:**1** ratio of 3.15:1 and undecane the lowest with 1.4:1. Outside of this group is 2,6-di-*tert*-butylphenol, with the lowest guest:**1** ratio of 0.7:1. These results are qualitatively in agreement with the values obtained by microcrystalline powder exchange, as the above guests were also detected in a range of about 1.5 to 3.0. Again, 2,6-di-*tert*-butylphenol is least absorbed, with a guest:**1** ratio of 0.6:1. These ratios indicate that all compounds investigated—aliphatic, nonfunctional aromatic, and aromatic alcoholic—are associated with **1**·AgOTf to an appreciable extent. Furthermore, while single crystal studies indicated a minimum of two benzene molecules for every molecule of **1**, these studies showed no presence of benzene, indicating that to the limits of detection by ^{1}H NMR all the benzene originally located crystallographically had been removed. The amount of toluene from the intermediate wash detected in the samples by ^{1}H NMR ranged from one to two molecules for every molecule of **1**.

While these ^{1}H NMR results indicate the presence of the guest molecule, the ratios obtained could be a consequence of surface adsorption rather than bulk inclusion. In order to determine the origin of these values, we examined the guest·**1**·AgOTf adducts by X-ray powder diffraction both before and after exchange.

Figure 2a shows the powder pattern calculated for all reflections from the single crystal data for **1**·AgOTf as originally grown in benzene. Figure 2b shows the powder pattern calculated for only 0*kl* reflections from **1**:AgOTf. It should be recalled that the 0*kl* reflections correspond to Bragg planes which have no *a* component in their normal vectors. Consequently, the Fourier transform of the 0*kl* planes corresponds to the projected electron density onto the *bc* plane of the original crystal (i.e., the real space plane which is normal to the *a** crystalline direction.) As may be seen in comparison of Figure 2 (parts a and b), a majority of the most intense reflections are in the 0*kl* plane (Table 2). Two of the strongest reflections in the calculated powder pattern are for the (002) and (011). In Figure 1c, we show these planes represented as real space plane waves for the 002 reflection. It may be seen that the (002) planes place most of the electron density of the well crystallized portion of the structure in phase. The relative intensity of this peak corresponds to the well crystallized host lattice as opposed to the much less well crystallized included solvent. The intensity of the 011 reflection can also be explained in a similar manner. The relative intensities of the 002 and 011 reflections, therefore, are a measure of the channel-like nature of the initial crystal structure. As we were unable to locate all solvent

Table 1. Solution Exchange Guest:**1** Molar Ratios and Unit Cell Parameters

			orthorhombic/rectangular unit cell parameters, Å		
guest[a]	macrocrystalline ratio	microcrystalline ratio	*a*	*b*	*c*
benzene single crystal			11.625(3)	19.110(7)	38.856(15)
toluene	1.47	1.9(2)	11.705(3)	19.29(2)	38.91(2)
m-xylene	2.31	1.97(8)	11.64(6)	19.58(3)	38.50(5)
undecane	1.42	1.27(2)	11.76(2)	19.231(9)	38.85(3)
benzyl alcohol	3.15	3.1(3)		22.43(1)	33.98(2)
(±)-phenethylalcohol	2.58	2.3(4)		22.49(1)	34.18(3)
2,6 di-*tert*-butylphenol[b]	0.73	0.60(5)		22.48(4)	32.84(4)
3-ethylphenol				21.98(2)	34.70(2)
phenol[c]				22.48(2)	34.08(6)
m-cresol				22.24(1)	34.51(2)
3,5 di-*tert*-butylphenol[b]				22.41(5)	33.87(7)
none				22.77(2)	36.32(4)

[a] Pure guest was used as solvent unless otherwise noted. [b] 3.0 M in benzene. [c] 5.4 M in benzene.

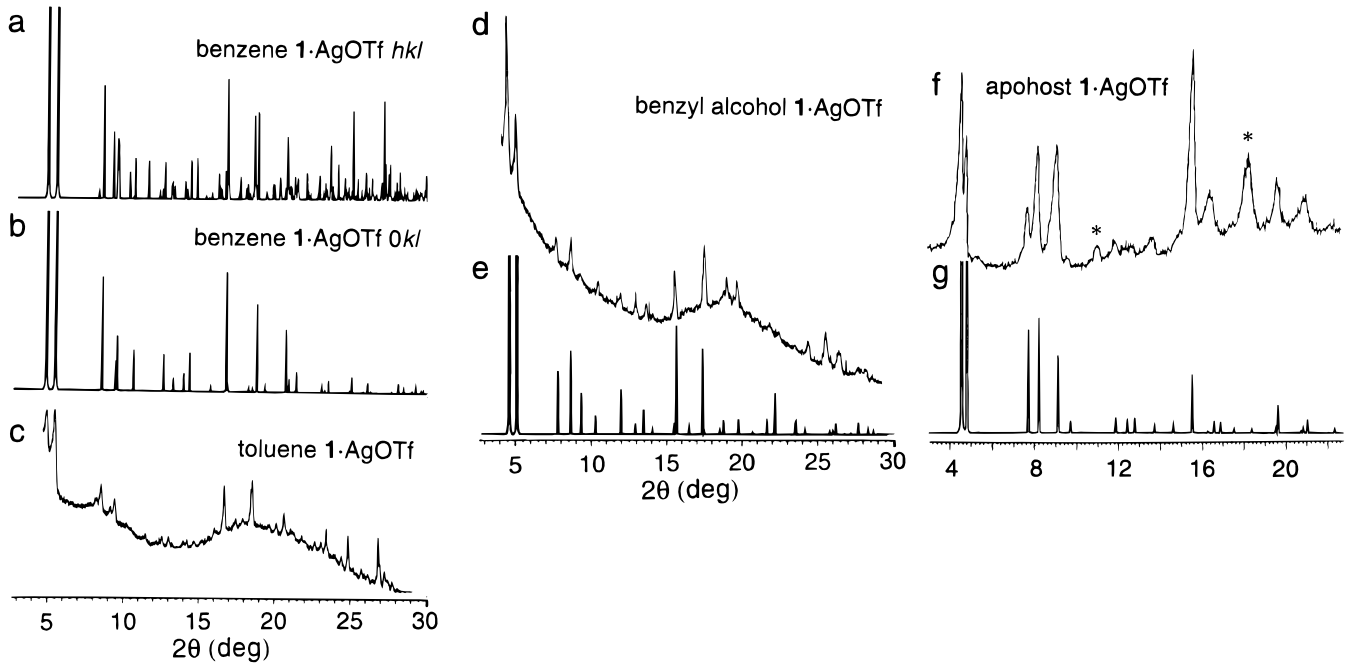

Figure 2. Calculated and observed single crystal *d*-spacings and intensities for the **1**·AgOTf structure. The intensities calculated for the 011 and 002 reflections have been reduced to conserve space. Relative intensities for these reflections are given in Tables 2 and 3. (a) The *hkl* powder pattern calculated for the benzene·**1**·AgOTf adduct. Crystal parameters are taken from the single crystal refinement. (b) the 0*kl* calculated powder pattern calculated from the single crystal parameters with included benzene. (c) Densitometer trace of the experimental Guinier powder pattern from the toluene·**1**·AgOTf adduct. (d) Densitometer trace of the experimental Guinier powder pattern from the benzyl alcohol·**1**·AgOTf adduct. (e) 0*kl* calculated powder pattern with the cell axes fitted to the unit cell parameters determined in Figure 2d. The original benzene·**1**·AgOTf single crystal fractional atomic positions are used without alteration. (f) Diffractometer trace of the powder pattern of apohost **1**·AgOTf where starred reflections are non-0*kl*. (g) 0*kl* powder pattern calculated with fitted cell axes from Figure 2f and the three parameter atomic refinement discussed in the text.

molecules in the structure, the calculated 002 and 011 intensities are overstated when compared with experiment.

Every nonalcoholic aromatic and aliphatic guest·**1**·AgOTf adduct listed in Table 1 exhibited a powder pattern similar to the calculated single crystal powder pattern (Figure 2c). The unit cell for these guests showed no variation greater than 0.4 Å of any cell axis from the original single crystal orthorhombic unit cell parameters (11.625(3) Å × 19.110(7) Å × 38.856(15) Å). A comparison of the Figure 2 (parts a and c) shows that the overall powder pattern of the toluene·**1**·AgOTf adduct retains most of the intense peaks found in the benzene sample. As comparison to Figure 2b shows, both 0*kl* and *hkl* ($h \neq 0$) reflections are found in the toluene samples. A detailed tabular comparison between the original benzene system and this nonalcoholic aromatic or aliphatic guest·**1**·AgOTf adducts is given in the supporting information. These data show that the principle features of the benzene·**1**·AgOTf adduct are retained with these nonalcoholic guests.

When the host was exposed to a solution of aromatic alcoholic guests, however, a different powder pattern from the original crystal was obtained, typified by the benzyl alcohol·**1**·AgOTf adduct shown in Figure 2d. In comparison with the original powder pattern for all *hkl* reflections shown in Figure 2a, Figure 2d possesses fewer reflections, and the patterns do not appear to be entirely similar. Comparison, though, between Figure 2 (parts b and d) illustrates a similarity between the 0*kl* reflections of the benzene and benzyl alcohol systems. We were able to index the reflections of the alcohol·**1**·AgOTf adduct by directly correlating them to the 0*kl* reflections of the original pattern, shown in Table 2, and by least squares fit obtaining new *b* and *c* parameters. The small margins of error between calculated and observed *d*-spacings in Table 2, the number of reflections indexed to number of parameters used, and the completeness of the indexation indicates this indexation is correct. Adjusting the unit cell parameters of the single crystal model to these new *b* and *c* axes, while not changing the fractional atomic positions,

Table 2. Observed and Calculated 0*kl* *d*-Spacings and Intensities up to 22° in 2θ for Benzyl Alcohol **1**·AgOTf

h	*k*	*l*	d_{obs}, Å	d_{calc}, Å	I_{obs}	I_{calc}
0	1	1	18.72	18.67	s	100
0	0	2	16.99	16.98	ms	69
0	2	0	11.21	11.21	wm	28
0	1	3	10.11	10.13	m	37
0	2	2	9.360	9.360	vw	18
0	0	4	*a*	8.495	vvw	8
0	3	1	7.296	7.296	wm	20
0	2	4	6.789	6.789	vvw	5
0	1	5	6.504	6.504	w	11
0	3	3	6.232	6.240	vw	2
0	0	6		5.663		5
0	4	0	5.607	5.611	s	49
0	4	2	5.325	5.332	vvw	3
0	2	6	5.055	5.063	m	39
0	3	5		5.029		2
0	1	7	4.741	4.744	vvw	2
0	4	4	4.680	4.669	vvw	6
0	5	1	4.447	4.449	vw	7
0	0	8		4.247		1
0	5	3		4.171		0
0	3	7	4.071	4.072	vvw	7

[a] Reflection too faint to accurately measure *d*-spacing.

resulted in the calculated powder pattern in Figure 2e. Reasonable agreement between observed and calculated intensities may be seen in Figure 2 (parts d and e). At higher θ values new reflections appear in the experimental powder pattern which can not be indexed as 0*kl* data. The first such reflection is at 26° in 2θ CuK$_{\alpha 1}$, corresponding to a *d*-spacing of 3.4 Å.

It is of interest to consider the origin of these unindexed reflections. This distance roughly corresponds to the interpenetrated net distance, along the *a* direction, of 3.5 Å. The original unit cell, with an *a* axis of 11.625(3) Å, spans three such $ThSi_2$-type networks. Two of these networks are crystallographically equivalent, and they sandwich the inequivalent third network between them. However, only a slight motion of the networks in the *bc* plane is necessary to make all nets crystallographically equivalent along the *a* direction (Figure 1b). Such net to net equivalency would then reduce the *a* unit cell parameter to merely the distance between networks. It is therefore attractive to suppose that the reflection observed at 26° corresponds not to a 0*kl* reflection but rather a *hkl* reflection ($h \neq 0$) and that the cell axis in the *a* direction has been reduced from the original 12 Å to the network interpenetration distance of about 3.5 Å. Unfortunately, there are insufficient potential *hkl* ($h \neq 0$) reflections to properly index the *a* axis. For this reason, we report only the *b* and *c* axis in Table 1. In any case, the fit of peak intensities of the 0*kl* reflections is reasonable up to 3.4 Å, after which the reflections are too faint to properly assign. Recalling from Figure 1b that the pores are 15 Å × 22 Å in dimension, this degree of resolution is sufficient to indicate the channel structure is preserved in the aromatic alcohol·**1**·AgOTf adduct.

Nearly all of the aromatic alcohol·**1**·AgOTf adducts in Table 1 can be indexed to the approximately same unit cell (about *b* = 22 Å, *c* = 34 Å) corresponding to a new pore dimension of 18 Å × 19 Å. The change in lattice parameters for these systems is indicative of a bulk effect, rather than a surface effect, in the method of guest/host association. We therefore conclude that even without guest:**1** molar ratios determined by ^{1}H NMR that overall bulk changes have occurred in all the aromatic alcohol·**1**·AgOTf adduct phases.

As an examination of Table 1 shows, the most significant changes in cell parameters are observed for aromatic alcoholic rather than for nonalcoholic systems. One possible rationalization of this observation lies with the hydroxyl oxygen of these alcohols. The oxygen may coordinatively bind to the silver cation, displacing the attracted triflate, and effect changes in the coordination sphere around the metal (Figure 3). It is known that the triflate counterion is only weakly coordinating, and it is expected that alcohols act as superior bases for the silver cation.

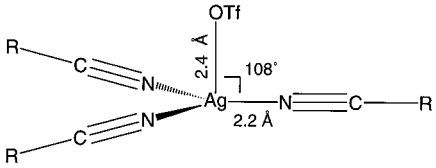

Figure 3. Coordination environment around a silver cation in **1**·AgOTf. The nitrile−silver bonds are 2.2 Å in length and lie roughly in a plane. The triflate anion (OTf) is coordinated on top of this plane to the silver at a distance of 2.4 Å. The three N−Ag−OTf bond angles vary from 84° to 137°. Overall, the fragment shown is approximately C_{3v} in symmetry.

We wish to highlight several control experiments designed to ensure the correctness of the data analysis:

(1) The Possibility of Recrystallization in Solution. As the exchange was carried out with the host lattice in direct contact with guests, solubility of the lattice in the solution could possibly lead to the dissolution and reformation of the crystal around the guest. The morphology of the crystalline habit was, therefore, monitored by optical microscopy under the conditions of the experiment.[27] The crystalline shape was observed to be constant throughout the duration of the experiment, with the exception of the crystals immersed in benzyl alcohol, which formed fibers extending from the exterior of the crystals. Even in this case, these growths were estimated to be less 1/100th of the volume of the main body of the crystals through the duration of the experiment and did not change the general appearance of the crystal.

(2) Necessity of Distinguishing between Guests Absorbed into the Host and Those Adsorbed onto the Surface of the Host. In order to use ^{1}H NMR to accurately determine included guest:**1** molar ratios, the incorporated guests had to be retained, and exterior, surface adsorbed guests had to be removed prior to analysis. This problem was addressed by subjecting the lattice exposed to the most viscous guests (all aromatic alcohols) to a wash with minimum amount of cold toluene. In addition, this washing was performed on both microcrystalline powder (0.03 mm × 0.01 mm × 0.01 mm) and macrocrystalline crystals (1 mm × 0.5 mm × 0.5 mm), and the relative guest:**1** molar ratios for these widely varying surface areas were found to be in reasonable agreement (Table 1).

(3) Verification That a Similar Nonporous Compound Shows No Absorption. For this comparison the crystalline compound chosen was the previously reported structure of the tritopic 1,3,5-tricyanobenzene with silver triflate.[4] No solvent is found in this structure, and there is no room for nondestructive accommodation of even the smallest molecule in the network.[28] The 1,3,5-tricyanobenzene·AgOTf crystalline powder, treated as described in the Experimental Section, by ^{1}H NMR exhibited the presence of any of the guests no greater than 0.03 molecules of the guest per molecule of 1,3,5-tricyanobenzene.

2. Removal of Guests from a Coordination Compound Host. The solution exchange studies discussed above suggested that the crystalline structure might be sufficiently resilient to survive complete removal of all guests in the channels.

(27) Examples of optical microscopy of the host crystal both before and after exchange are included in the supplementary materials.

(28) Spek, A. L. *J. Appl. Crystallogr.* **1988**, *21*, 578−579.

Consequently, a TGA apparatus was used to remove the included solvent quickly and to estimate the total amount of benzene originally present.[29] Weight loss by this method corresponded to approximately three benzenes for every **1**·AgOTf unit, shown in Figure 4. The recovered material after analysis was a lightly browned powder. By ^{1}H NMR, the organic ligand remained intact, and the ratio of benzene:**1** was found to be <0.1:1. CHN analysis was compatible with **1**·AgOTf.[30] As no foreign guest could be detected by ^{1}H NMR in these latter crystals, we designate this guest-free material as an apohost.

The X-ray powder pattern obtained from **1**·AgOTf after heating to 200 °C is shown in Figure 2f. By inspection, the powder pattern from the material subjected to thermal evacuation bears a number of similarities to the patterns obtained by alcohol solution exchange, specifically, the retention and displacement in θ of only the most intense reflections. Consequently, we indexed the powder pattern as 0*kl* reflections in an analysis similar to that used for the aromatic alcohol systems. The refined and observed reflections are shown in Table 2. The resulting rectangular unit cell parameters, $b = 22.77(2)$ Å, $c = 36.32(4)$ Å (Table 1), describe an area similar to the that of the aromatic alcohol·**1**·AgOTf adducts. The cell axes of both the apohost and the aromatic alcohol systems show a similar deformation relative to the original orthorhombic unit cell; there is an elongation along the *b* axis and a contraction along the *a* axis. The small error between calculated and observed *d*-spacings (Table 3), the small number of refined parameters and the completeness of the indexation lead us to conclude that this indexation is correct.

The evaporation of all guests places more stringent demands on the host than the solution exchange of guests. We therefore examined if the two-dimensional model used for the aromatic alcohol·**1**·AgOTf adduct could also plausibly explain the observed intensities of the apohost 0*kl* reflections. Such a refinement would utilize all 0*kl* reflections up to the largest observed θ value, the (0 2 10), corresponding to a *d*-spacing of 3.46 Å. From the determined unit cell axes, there are a total of 31 0*kl* reflections which are calculated to have this or a lower *d*-spacing value, of which half are observed and half are unobserved. Allowing a reasonable data to parameter ratio, these 31 calculated reflections permits at most the introduction of three parameters to the original single crystal model to explain the diffraction pattern. Given the few parameters, it was necessary to treat the constituent molecules as near rigid bodies.

Inspection of the crystal structure reveals that there are three separate $ThSi_2$-type networks in the unit cell. Allowing translational motion for each net leads to potentially six parameters in the refinement of the two-dimensional unit crystal structure projection (recall that no net has a covalent bond to another net). However, the nets lie in special positions, as shown in Figure 1, where they are bisected by a mirror plane normal to the *b* axis. This symmetry reduces the number of possible translations of the networks from six to three. The total number of parameters is further reduced as two of the networks are crystallographically equivalent. Translation of one of these nets results in an identical translation of the other, and this limits the number of parameters to two. Finally, as one translation of the one inequivalent net is identical with an opposite translation of the two symmetry related nets, only one movement of the networks is allowed and there remains only a single translational parameter. We find a best fit in this refinement corresponds to a shift of the inequivalent network along the *c* axis by 1.5 Å relative to the two symmetry equivalent nets. The only remaining structural features in the apohost cell are the triflate counterions. There are two crystallographically inequivalent triflate anions, one lying on the orthorhombic mirror plane and the other in a more general position away from this plane. The anion on the mirror plane has its central carbon−sulfur vector along the *c* axis and in line with the networks. Because this anion lies on the same symmetry plane as the networks, it was treated as part of the rigid body and translated as part of the nets. There are no remaining motions allowed to this triflate other than rotation around the carbon−sulfur axis, a change too small to effect the large Å resolution of this refinement. Our attention therefore turned to the remaining triflates. Unlike the $ThSi_2$-type networks, both rotational and translational motion of the anions are compatible with the space group and crystal structure type. If all rotational and translational motions are allowed, this introduces four parameters, too many for the small number of reflections used in the refinement. We therefore selected a single rotational parameter, corresponding to a rotational axis parallel to the *c* axis, and defined a single translational motion between the *b* and *c* axes. We chose the former as it corresponds to the greatest possible change in the two-dimensional projected electron density and the latter as it allows the triflate to return to a equal distance between neighboring phenyl rings of the displaced networks. We find a good agreement for a rotation of 90° along the *c* axis and a displacement in the *bc* direction by 0.6 Å.

It is important to note that the three parameters used to describe the translations and rotations performed are chemically reasonable. Motion of one net in the *a* or *b* directions causes bonds in adjacent networks to cross and introduces unreasonably close $\pi-\pi$ interactions. However, translation in the *c* direction not only preserves the connectivity of the lattice by not breaking any bonds but also maintains the space between networks at 3.5 Å. Rotation and translation of the triflate anion causes no unfavorable close contacts and places the anion 3 Å from the silver cation. In the single crystal, the oxygen atoms of the triflate counterions are located 2.4 and 3.7 Å from the silver atoms, suggesting that this final distance is a reasonable one.

The calculated powder pattern of the structure following these alterations is shown in Figure 2g. Note the reasonable agreement in calculated and observed intensities between Figure 2 (parts f and g). A numerical comparison is given in Table 3. As with the previous two-dimensional solution, the intensity present up to the lowest indexed 0*kl* can be used as a measure of the resolution obtained, in this case corresponding to a *d*-spacing of 3.5 Å. Recalling that the pore size of the original crystal at 15 Å × 22 Å, 3.5 Å resolution is enough to insure that the channel structure is retained through revaporation of the initially included guests.

As with the aromatic alcohol·**1**·AgOTf adduct, there are relatively high 2θ $CuK_{\alpha 1}$ reflections experimentally observed which are not accounted for in the 0*kl* model. The reflections with the smallest 2θ value clearly observed which cannot be indexed in the two-dimensional model occur at 9.6° and 18.2°. In the aromatic alcohol model, we had suggested that the lowest unindexed reflection, with a *d*-spacing of 3.95 Å, corresponded to the new network-to-network distance along the *a* axis. Similarly, the unindexed reflections in the apohost may arise from *hkl* ($h \neq 0$) reflections, although it is reasonable that these may also be due to the formation of a second product. In any

(29) Measurement by this technique was complicated by the difficulty of "drying" the sample so the slowly evaporating included benzene would remain with the sample while benzene on the exterior of the channels would be excluded from the initial weight. It was decided that a lower bound could be obtained by measuring the sample after the powder itself appeared dry.

(30) Anal. Calcd for $C_{35}H_{15}N_3AgO_3SF_3$: C, 57.46; H, 2.44; N, 5.63; Ag, 15.2. Found: C, 56.16; H, 2.44; N, 5.63; Ag, 14.5.

Table 3. Observed and Calculated 0*kl* *d*-Spacings and Intensities up to 25.8° in 2θ for Apohost **1**·AgOTf

h	*k*	*l*	d_{obs} Å	d_{calc} Å	I_{obs}	I_{calc}
0	1	1	19.49	19.29	m	1000
0	0	2	18.17	18.16	w	277
0	2	0	11.41	11.38	vw	45
0	1	3	10.71	10.69	w	50
0	2	2	9.657	9.645	wm	34
0	0	4	9.129	9.079	vvw	5
0	3	1	7.431	7.429	vvw	7
0	2	4	6.998	7.098	vvw	6
0	1	5		6.920		7
0	3	3	6.446	6.430	vvw	3
0	0	6		6.053		4
0	4	0	5.694	5.692	m	26
0	4	2		5.431		1
0	2	6	5.363	5.344	vw	5
0	3	5		5.247		5
0	1	7		5.058		2
0	4	4		4.823		2
0	0	8		4.540		2
0	5	1	4.519	4.518	w	12
0	3	7		4.283		1
0	5	3		4.262		2
0	2	8	4.228	4.217	vvw	6
0	4	6		4.147		0
0	1	9		3.973		2
0	5	5		3.858		2
0	6	0	3.789	3.795	w	3
0	6	2		3.715		0
0	0	10		3.632		1
0	3	9		3.563		5
0	4	8		3.549		1
0	6	4		3.501		0
0	2	10	3.456	3.460	vvw	5

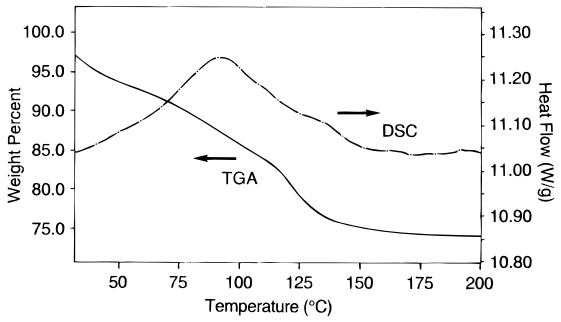

Figure 4. TGA and DSC traces of the benzene·**1**·AgOTf adduct, each recorded at a heating rate of 10 °C/min.

case, there are insufficient reflections to properly index the *a* axis. Consequently, only the *b* and *c* axes are reported.

The 011 and 002 reflections, previously noted in connection with the channel structure (Figure 1c), are observed to be somewhat diminished in intensity relative to the calculated powder pattern. The attenuation of this observed intensity is indicative of introduction of electron density between these planes and into the channels themselves. As only the reflections at lowest θ values are affected, the electron density corresponding to this diminuation of intensity must be material which is highly disordered and possesses large thermal factors. During the synthesis of the apohost, one can imagine the material generated during the thermal procedure collecting in the evacuated pores. As will be shown, however, this introduction of material into the cavities does not irreversibly seal the channels to the introduction of other guests.

Additional evidence for maintenance of the $ThSi_2$-type structure comes from the TGA/DSC traces. The most significant loss in weight by TGA occurs before 130 °C (Figure 4). In comparison, the open pan DSC of this material shows a broad and substantial feature between 50 and 150 °C with no other significant activity up to 200 °C. The shape of the broad peak is not characteristic of a phase change but rather with the process of evaporating solvent. Furthermore, the DSC parallels the TGA weight loss almost exactly, suggesting that what is observed in the DSC is the endothermic loss of benzene. The absence of a phase transition suggests that the network connectivity is maintained during and after the liberation of guests, allowing for the preservation of the integrity of the channel structure.

3. Guest Introduction into a Voided Porous Coordination Solid. Indication that **1**·AgOTf had retained its crystal structure despite complete loss of included molecules prompted investigations into the possibility of reintroduction of guest molecules into the apohost by means of vapor transport. Absorption data for apohost **1**·AgOTf is shown in Table 4. The guest molecules most absorbed were benzyl alcohol and (±)-*sec*-phenethyl alcohol with guest:·**1**·AgOTf ratios of 3.62:1 and 3.52:1, respectively. Somewhat less absorbed were the nonfunctionalized aromatics benzene and *m*-xylene with guest:**1**·AgOTf ratios of 2.51:1 and 1.28:1 respectively. All nonaromatic guests investigated showed an absorption ratio of less than 0.15:1 guest:**1**·AgOTf, with undecane having the highest ratio of 0.11:1. Consideration of boiling points of the guests in Table 4 demonstrates that this selectivity was not simply an effect of the molecular population in the gas phase. The highest boiling compound, (±)-*sec*-phenethyl alcohol (bp 225 °C), was one of the most absorbed, while the much lower boiling cyclooctane (bp 155 °C) was essentially not absorbed.

Consideration of the original crystal structure suggests an origin for the observed selectivity. The walls of the channels, primarily composed of phenylacetylene ligands, are aromatic in nature. In the benzene·**1**·AgOTf structure, benzene molecules are located inside this channel, suggesting that inclusion of these aromatic guests is energetically favorable. The absorption of other aromatic molecules, such as toluene and *m*-xylene, seems attributable to the same effect. Conversely, the almost undetectable absorption of the aliphatic molecules suggests that the primarily aromatic cavities are intolerant of these nonaromatic molecules. The relatively large absorption ratio for aromatic alcoholic guests may be due to not only the aromatic nature of the guest but also the hyroxyl alcohol, which, as postulated before, may coordinatively bind to the silver cation (Figure 4).

X-ray powder patterns of the host were taken both before and after exposure to the guest in the vapor phase, as shown in Table 4. The vapor transport powder pattern for the aromatic alcoholic·**1**·AgOTf adducts could be indexed to the previously discussed two-dimensional rectangular cell and determined to be within 0.4 Å of their solution exchange counterparts. The benzene·**1**·AgOTf readopted the *hkl* pattern of the single crystal powder pattern and the orthorhombic unit cell parameters could be indexed within 0.4 Å of the original unit cell parameters. The *m*-xylene·**1**·AgOTf adduct could be indexed to a two-dimensional rectangular cell of $b = 21.87(5)$ and $c = 34.65(9)$, close to the aromatic alcoholic·**1**·AgOTf adduct parameters. As expected, nonaromatic molecules, which were not absorbed, did not change the apohost parameters by more than 0.3 Å from the original rectangular unit cell.

Resubmission of the benzyl alcohol·**1**·AgOTf adduct to TGA regenerated the apohost powder pattern. Through three successive exposures to benzyl alcohol and subsequent generation of the apohost, TGA indicated that the amount of guest absorbed was constant at 3.5 guests per unit of **1**·AgOTf, shown in Figure 5. The temperature required to remove the guests after successive cycles, however, decreased steadily, with consecutive points of steepest descent occurring at 141, 136, and 131 °C.

Table 4. Vapor Transport Guest:**1** Ratios and Unit Cell Parameters

				orthorhombic/rectangular unit cell parameters, Å		
guest[a]	bp, °C	exposure, h	guest:**1** ratio	*a*	*b*	*c*
none					22.77(2)	36.32(4)
benzene	80	24	2.52(5)	11.353(5)	19.07(3)	39.15(3)
m-xylene	138	36	1.28(4)		21.87(5)	34.65(9)
cyclooctane	155	12	0.063(6)		22.591(8)	36.02(8)
decahydronapthalene	193	12	0.07(0)		22.925(8)	36.635(23)
undecane	196	24	0.113(6)		22.867(6)	36.533(7)
benzyl alcohol	205	12	3.62(3)		22.393(12)	34.138(14)
(±)-*sec*-phenethyl alcohol	225	12	3.5(1)		22.319(7)	34.42(2)

[a] All exposures were carried out at 60 °C, with the exception of benzene, which was included at 40 °C.

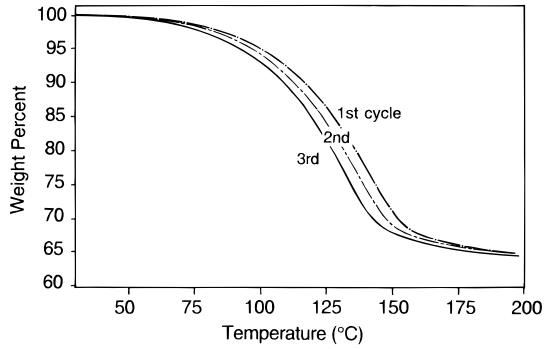

Figure 5. TGA traces of the benzyl alcohol·**1**·AgOTf adduct formed by repeatedly exposing the apohost **1**·AgOTf to benzyl alcohol in the vapor phase and then thermally removing the guests. Points of steepest descent occur at 141, 136, and 131 °C for the first, second, and third cycles, respectively. The weight loss in each case corresponds to 3.5 molecules of benzyl alcohol for every **1**·AgOTf.

This indication of the progressive weakening of the guest/host interaction suggests that the structure, through the repetition of heating, is slowly being degraded. However, even after the third cycle of exposure to vapor and thermal evacuation, the material was crystalline and could be indexed to the apohost rectangular cell parameters. This readoption of cell parameters and intensities demonstrates that through multiple exposures to and removals of guests the $ThSi_2$-type structure is maintained.

Several controls on the vapor exchange were carried out. The crystalline powder was optically monitored, and no morphology change over the course of the experiment was observed with the exception of benzene, which formed small needlelike crystallites. In a second set of control experiments, the apohost was heated at 65 °C without guests present to determine if a phase change occurred over the duration of the experiment. Apohost material treated in this manner exhibited an identical powder pattern to that of the original **1**·AgOTf apohost.

Conclusion

In zeolites a host structure is capable of guest evacuation and exchange without destruction of the network connectivity. The three-dimensional coordination compound **1**·AgOTf exhibits these same properties. It can be "calcined" at 200 °C to form an apohost voided of initially included benzene. Verification of the original structure comes from powder diffraction and TGA/DSC studies. The apohost can absorb guests from the vapor phase with selectivity, showing preference for aromatic alcohols and to a lesser extent unfunctionalized aromatics over aliphatic molecules. Verification that the vapor exchange structure is that of the solution exchange structure arises from their identical powder patterns. The host adduct can be repeatedly voided of and filled with guest molecules without the destruction of the $ThSi_2$-type network. In addition, **1**·AgOTf functions as a host for a variety of guest molecules in solution without observable destruction of the crystalline morphology. The powder patterns for these new guest·**1**·AgOTf adducts are characteristic and reasonably match in intensity the calculated diffraction pattern from the single crystal model.

Acknowledgment. We gratefully thank Professor Jeffrey S. Moore for his critical evaluation of this manuscript and steady support and encouragement throughout the execution of this work. We thank Professor Thomas Dunn for use of his densitometer and Professors. B. J. Evans, Dave Martin, and Michael Morris for the use of their optical microscopes. Financial support comes from the National Science Foundation (Grant CHE-94-23121). Fellowship from the A. P. Sloan Foundation (1993−1995) and the J. D. and C. T. MacArthur Foundation (1993−97) are gratefully acknowledged. This paper is dedicated to Prof. Dr. Wolfgang Jeitschko on the occasion of his 60th birthday.

Supporting Information Available: Tables containing diffraction data for solution exchange and vapor transport exchange crystals as well as optical microscopy photographs of crystals in solution exchange (9 pages). See any current masthead page for ordering and Internet access instructions.

JA960595R